3-19-96

SAND96-0791C
CONF-9606115--3

EVALUATION OF CONSTITUTIVE MODELS FOR CRUSHED SALT

Gary D. Callahan
Marc C. Loken
RE/SPEC Inc., Rapid City, SD 57701

L. Diane Hurtado
Frank D. Hansen
Sandia National Laboratories, Albuquerque, NM 87185

ABSTRACT

Three constitutive models are recommended as candidate constitutive models to describe the deformation of crushed salt. The candidate constitutive models are generalized to three-dimensional states of stress to include the effects of mean and deviatoric stress and modified to include the effects of temperature, grain size, and moisture content. A database including hydrostatic consolidation and shear consolidation tests conducted on Waste Isolation Pilot Plant (WIPP) and southeastern New Mexico salt is used to determine material parameters for the candidate constitutive models. To evaluate the capability of the candidate models, the parameter values obtained from fitting the complete database are used to predict the individual tests. Finite element calculations of a WIPP shaft with emplaced crushed salt demonstrate the model predictions.

INTRODUCTION

The Waste Isolation Pilot Plant (WIPP) is designed as the first full-scale, mined geological repository for the safe management, storage, and disposal of transuranic (TRU) radioactive wastes generated by the Department of Energy (DOE) defense programs. The WIPP underground facility, located in southeastern New Mexico at a depth of approximately 655 m in bedded halite, consists of a series of underground shafts, drifts, panels, and disposal rooms. After the facility meets the requirements of the Environmental Protection Agency (EPA), each disposal room will be filled with containers holding TRU wastes of various forms. Ultimately, a seal system will be emplaced to prevent water from entering the repository and to prevent gases and brines from migrating out of the repository.

Crushed salt has been proposed as a key component material for permanent sealing of WIPP underground openings. Crushed salt's desirable characteristics include chemical compatibility, eventual mechanical similarity with the host salt formation, and availability from the site excavation. In addition, voids in crushed salt close and heal in response to applied loads. Laboratory tests have shown that crushed salt achieves desirable permeability characteristics as consolidation increases the material density.

An understanding of consolidation processes in crushed salt is fundamental to the design of a credible seal system that will provide confidence in establishing regulatory compliance. The objective of this paper is to examine the mechanical material models appropriate for describing crushed-salt deformation.

To meet our objective, the study was divided into five major parts: (1) literature review and candidate model selection, (2) three-dimensional generalization of the candidate models, (3) assembly of an experimental database to evaluate material parameters for the candidate models, (4) nonlinear least-squares fitting of the candidate models to the database and evaluation of the statistics, and (5) implementation of the models into a finite element code and demonstration of model response for a typical in situ problem. Each of these activities are discussed separately in the remainder of this paper.

LITERATURE REVIEW

A review of the literature was conducted to identify existing models used to describe deformation of crushed salt and to determine mechanisms governing the deformation processes. From this review, candidate models were selected that are mechanism-based and representative of the range of conditions expected at the WIPP.

From a phenomenological viewpoint, the mechanical behavior of crushed salt can be divided into elastic, plastic, and viscoplastic deformation. The various models governing the phenomenological behavior may be divided into time-independent and time-dependent deformation. Time-independent densification of crushed salt includes particle rearrangement, cataclasis, and plastic yield. Time-dependent densification of crushed salt includes dislocation creep and pressure solutioning. Densification or consolidation of crushed salt depends strongly on particle size and moisture content with the rate of deformation increasing rapidly as particle size decreases and moisture content increases. Added moisture activates the pressure solution processes characterized by material dissolution-precipitation induced by stressing along the intergranular brine.

Ten crushed-salt constitutive models were identified from the literature search described by Callahan et al. [1995]. Essentially, these constitutive models were developed to reproduce hydrostatic (isostatic) consolidation laboratory tests and include only the volumetric strain component. However, in recent years, deviatoric stresses have been recognized to influence consolidation in the crystalline powder industry (e.g., Xu and McMeeking [1995]). Whether or not deviatoric stresses assist in the consolidation processes of crushed salt, inclusion of the component is necessary to be able to describe the distortion of the crushed salt in general and make any model acceptable for performing numerical simulations.

From the ten models identified, three were selected as candidate models for further examination. The three candidate models are those attributable to Sjaardema and Krieg [1987], Zeuch [1990], and Spiers and Brzesowsky [1993]. The Sjaardema and Krieg model is empirical and was retained for comparative purposes since it has been used in the past for calculation of crushed-salt problems at the WIPP. The Zeuch model was constructed for nominally dry crushed salt and is based on isostatic hot-pressing models

and dislocation creep. The Spiers model was formulated for wet crushed-salt aggregates and is based on grain boundary diffusional pressure solution processes.

CANDIDATE CONSTITUTIVE MODELS

This section presents the general form of the crushed-salt constitutive model and development of the three-dimensional generalization for the candidate constitutive models. An empirical function containing the effects of moisture, particle size, and temperature is included, which modifies the equivalent inelastic strain rates defined by the candidate models.

General Constitutive Model Form

The total strain rate for the crushed-salt constitutive model is assumed to consist of three components. The components include nonlinear elastic ($\dot{\varepsilon}^e_{ij}$), consolidation ($\dot{\varepsilon}^c_{ij}$), and creep ($\dot{\varepsilon}^i_{ij}$) contributions, and the total strain rate is written as the sum of these rates:

$$\dot{\varepsilon}_{ij} = \dot{\varepsilon}^e_{ij} + \dot{\varepsilon}^c_{ij} + \dot{\varepsilon}^i_{ij} \tag{1}$$

Both the nonlinear elastic and consolidation portions of the model describe the material behavior in bulk (volumetric) and in shear (deviatoric). However, the creep portion of the model only describes deviatoric material behavior and is, in fact, the creep deformation model used for intact salt. The nonlinear elastic model adopted is that given by Sjaardema and Krieg [1987]. The creep portion of the model is described by Munson et al. [1989].

Consolidation Model

The consolidation model is of primary concern in this study, and thus, this section is divided into subsections that address important issues regarding the consolidation portion of the crushed-salt model. Typically, equations proposed to describe the behavior of a particular material are written in one-dimensional form or as scalar relationships. To be useful in numerical analyses and applicable to a variety of laboratory experiments with different load paths, any constitutive model must be generalized to include three-dimensional states of stress. The first subsection presents the generalization of the candidate constitutive model forms. The next subsection presents considerations for moisture, particle size, and temperature effects on the deformation of crushed salt. Since no single model includes all of these state variables, an empirical function is proposed to include their influence in the models. The last subsection presents the candidate constitutive model forms as modified to capture the phenomena associated with the crushed-salt creep component of the constitutive model.

Consolidation Model Generalization

Following the approach of Fossum et al. [1988], the three-dimensional generalization of the kinetic equation for the consolidation inelastic flow is:

$$\dot{\varepsilon}^c_{ij} = \dot{\varepsilon}^c_{eq}\left(\sigma^f_{eq}\right)\frac{\partial \sigma_{eq}}{\partial \sigma_{ij}} \tag{2}$$

where $\dot{\varepsilon}^c_{ij}$ is the inelastic strain rate tensor and σ^f_{eq} and $\dot{\varepsilon}^c_{eq}$ are the power-conjugate equivalent stress measure and equivalent inelastic strain rate measure for creep consolidation, respectively; and the equivalent inelastic strain rate measure is written as a function of the equivalent stress measure. For use in the flow potential, another equivalent stress measure, σ_{eq}, is used to provide a nonassociative formulation that provides flexibility in governing the magnitude of the volumetric behavior.

Motivation for selection of the equivalent stress measures comes from laboratory experiments. Tests on crushed-salt specimens exhibit a strong dependence on the pressure (mean stress) applied to the specimens. Shear consolidation experiments also exhibit differing behavior, depending on the magnitude of applied stress difference. In fact, the lateral strain in a typical triaxial test may be either positive or negative, depending on the relative magnitudes of the mean stress, stress difference, and the material's density. Thus, the appropriate stress measure should include both mean and deviatoric stress and density dependencies. Laboratory tests on *intact* salt specimens show little dependence on moderate mean stress levels (>2 MPa), and typically, the deformation of intact salt is described as a volume-preserving process. Therefore, one would expect the mean stress influence to decrease as the crushed salt approaches full consolidation. With these considerations, the equivalent stress measures are given by:

$$\begin{aligned}
\sigma^f_{eq} &= \eta\left|\sigma_m\right|^{\eta_2} - \frac{\left|\sigma_1 - \sigma_3\right|^{m_1}}{\sigma_{r_1}^{m_1-1}} \\
\sigma_{eq} &= \kappa\left|\sigma_m\right|^{\kappa_2} - \frac{\left|\sigma_1 - \sigma_3\right|^{m_2}}{\sigma_{r_2}^{m_2-1}}
\end{aligned} \tag{3}$$

where:

$\eta = \eta_0(1 - \Omega)^{\eta_1}$

$\kappa = \kappa_0(1 - \Omega)^{\kappa_1}$

$$\Omega = \begin{cases} D_t, & D < D_t \\ D, & D \geq D_t \end{cases}$$

D_t = transitional fractional density

D = fractional density

σ_m = mean stress

σ_1, σ_3 = principal stresses

σ_{r_1}, σ_{r_2} = reference stresses

η_0, η_1, η_2, κ_0, κ_1, κ_2, m_1, and m_2 = material parameters.

The equivalent stress measure (σ^f_{eq}) is defined to be a negative quantity for compressive states of stress that drive the consolidation processes, which requires that η_0 be positive. As the crushed salt approaches full consolidation, η and κ approach zero, and the mean stress dependency diminishes. Twice the maximum shear stress or the Tresca equivalent stress is used in the equivalent stress measures to describe the shear behavior and is given by:

$$|\sigma_1 - \sigma_3| = 2\cos\psi\sqrt{J_2} \tag{4}$$

where the Lode angle (ψ), which is a convenient alternative invariant to J_3, is given by:

$$\psi = \frac{1}{3}\sin^{-1}\left[\frac{-3\sqrt{3}\,J_3}{2J_2^{3/2}}\right], \left(-\frac{\pi}{6} \le \psi \le \frac{\pi}{6}\right) \tag{5}$$

with the second and third invariants of the deviator stress (s_{ij}) defined by:

$$J_2 = \frac{1}{2}s_{ij}s_{ji} \qquad J_3 = \frac{1}{3}s_{ij}s_{jk}s_{ki} \tag{6}$$

The partial derivative given in Equation 2 may be determined using the chain rule as:

$$\frac{\partial\sigma_{eq}}{\partial\sigma_{ij}} = \frac{\partial\sigma_{eq}}{\partial\sigma_m}\frac{\partial\sigma_m}{\partial\sigma_{ij}} + \frac{\partial\sigma_{eq}}{\partial J_2}\frac{\partial J_2}{\partial\sigma_{ij}} + \frac{\partial\sigma_{eq}}{\partial\psi}\frac{\partial\psi}{\partial J_3}\frac{\partial J_3}{\partial\sigma_{ij}} \tag{7}$$

Performing the differentiation and substituting Equation 7 into Equation 2 provides the tensorial strain rate components for the consolidation portion of the crushed-salt model, which is given by:

$$\dot{\varepsilon}^c_{ij} = \dot{\varepsilon}^c_{eq}\left\{\frac{\kappa\kappa_2|\sigma_m|^{\kappa_2-1}}{3}\delta_{ij} - \frac{m_2}{\sigma_{r_2}^{m_2-1}}\left(2\cos\psi\sqrt{J_2}\right)^{m_2-1}\left(\left[\frac{\cos 2\psi}{\cos 3\psi}\right]\frac{s_{ij}}{\sqrt{J_2}} + \left[\frac{\sqrt{3}\sin\psi}{J_2\cos 3\psi}\right]t_{ij}\right)\right\} \tag{8}$$

where $t_{ij} = s_{ik}s_{kj} - \frac{2}{3}J_2\,\delta_{ij}$.

The flow potential contains five material parameters (κ_0, κ_1, κ_2, σ_{r_2}, and m_2) that need to be determined from laboratory experiments. To complete the crushed-salt creep consolidation description, the equivalent inelastic strain rate (kinetic equation) for the crushed-salt model needs to be defined. The kinetic equations are the three specific crushed-salt models selected from the literature review.

Moisture-Particle Size-Temperature Function

The addition of a small amount of moisture significantly increases the consolidation rate of crushed salt. In addition, there appears to be a quantity of moisture above which further increases in the consolidation rate are not noticeable. However, the amount of moisture producing the largest consolidation rate may vary depending on temperature and pressure. When a significant amount of moisture is available, a retardation in the consolidation rate could occur if the interconnected porosity disappears and the moisture is trapped leading to the generation of pore pressures. Researchers find that particle size or grain-size dependency is inversely proportional to the cube of the average grain-size diameter. Grain size is believed to be more important when moisture is present because densification through pressure solutioning is operative. Crushed-salt consoli-

dation rates have been observed to increase with increasing temperature. This most likely occurs because of the thermally activated dislocation motion within the crushed-salt particles. Most researchers have adopted the same temperature-dependent forms for crushed salt and intact salt, and the same form is used here.

The effects of moisture, particle size, and temperature are combined to form parameter (ξ), which is incorporated as a multiplicative constant on the equivalent inelastic strain rate:

$$\xi = \frac{L}{d^p}\left[1 + a_1\left(1 - \exp\left(-a_2 w\right)\right)\right]\exp\left(-\frac{Q_c}{RT}\right) \tag{9}$$

where:

w = moisture fraction by weight

a_1, a_2 = material parameters

d = average grain diameter [m]

p = material parameter

L = dimensional parameter [m ^{p}]

R = universal gas constant $\left[\frac{J}{\text{mol-K}}\right]$

T = absolute temperature [K]

Q_c = material parameter $\left[\frac{J}{\text{mol}}\right]$

Equivalent Inelastic Strain-Rate Forms

Three different equivalent inelastic strain-rate forms are used to describe the consolidation portion of the crushed-salt material model, including:

- Sjaardema and Krieg Empirical Model [Sjaardema and Krieg, 1987].
- Zeuch's Isostatic Hot-Pressing Model [Zeuch, 1990].
- Spiers' Pressure Solution Model [Spiers and Brzesowsky, 1993].

Each of these functional forms is presented below in terms of true or logarithmic strain (e). In all instances, compaction/consolidation strain and compressive stress are assumed to be negative. The use of this sign convention results in sign changes from the original referenced models. In addition, multiplicative constants have been combined into a single constant. Moisture, temperature, and particle size dependencies are included using the function described in Equation 9, which adds four material parameters to each of the models (i.e., p, a_1, a_2, and Q_c). The effective stress measure in Equation 3 describing the flow potential adds five material parameters to each model: κ_0, κ_1, κ_2, σ_{r_2}, and m_2.

The modified Sjaardema and Krieg model is written as:

$$\dot{e}^{c}_{eq} = \xi\,\frac{B_0\exp(e_v)}{\rho_0}\,\sigma^{f}_{eq}\exp\left[A\rho_0\exp\left(-e_v\right)\right] \tag{10}$$

The modified Sjaardema–Krieg model has eight material constants – η_0, η_1, η_2, D_t, m_1, σ_{r_1}, B_0, and A.

The modified Zeuch isostatic hot-pressing model is written for two stages, depending on the fractional density, as:

For Stage 1 ($D_0 \le D \le 0.9$):

$$\dot{e}_{eq}^{c} = \xi\, b_7 D_0^{b_2} D^{2(b_2-n)-1} \left(\frac{D - D_0}{1 - D_0} \right)^{b_3-n} \sigma_{eq}^{f} \tag{11}$$

For Stage 2 ($0.9 < D \le 1$):

$$\dot{e}_{eq}^{c} = \xi\, b_8 \frac{(1 - D)}{\left\{1 - (1 - D)^{1/n}\right\}^{n}} \sigma_{eq}^{f} \tag{12}$$

where $D = D_0 / \exp(e_v)$. The modified Zeuch model requires an original value of fractional density (D_0) that is less than the initial fractional density value; otherwise, the strain rate is always zero, as shown in Equation 11. Thus, a value of $D_0 = 0.64$ is typically used, which represents the theoretical value for identical-sized spheres. The modified Zeuch model has eleven material constants – η_0, η_1, η_2, D_t, m_1, σ_{r_1}, b_2, b_3, b_7, b_8, and n.

The grain boundary pressure solution model presented by Spiers can be indeterminate since when $\sigma_{eq}^{f} = 0$, the initial volumetric strain is zero. To eliminate this problem, an initial volumetric strain is assumed, $e_{v_0} = \ln(D_0/D_i)$, where D_0 is assumed to be 0.64 and D_i is the initial fractional density. With this change, the modified Spiers pressure solution model is written in terms of a volumetric strain component defined as $e_v^* = e_v + e_{v_0}$.

$$\dot{e}_{eq}^{c} = \xi\, r_1 \exp\left(-e_v^*\right) \left(\frac{\exp\left(r_3 e_v^*\right)}{\left|\exp\left(e_v^*\right) - 1\right|^{r_4}} \right) \Gamma\, \sigma_{eq}^{f} \tag{13}$$

where Γ is given by:

$$\Gamma = \begin{cases} 1 & \text{small strain } \left(\exp\left(e_v^*\right) - 1 > -15\%\right) \\ \left[\dfrac{\exp\left(e_v^*\right) + \phi_0 - 1}{\phi_0 \exp\left(e_v^*\right)} \right]^{n} & \text{large strain } \left(\exp\left(e_v^*\right) - 1 < -15\%\right) \end{cases} \tag{14}$$

where ϕ_0 is the initial porosity. The modified Spiers model has ten material constants – η_0, η_1, η_2, D_t, m_1, σ_{r_1}, r_1, r_3, r_4, and n.

EXPERIMENTAL DATABASE

A data assessment was performed to identify appropriate data for WIPP crushed-salt model development. The data assessment was performed by establishing acceptance criteria, which included:

- Crushed-salt source: WIPP or other southeastern New Mexico sites.
- Bentonite content: 0 percent (by weight).
- Temperature: 293K to 373K.
- Grain size: <10 mm.
- Specimen size: >80 mm (in diameter).
- Moisture content: 0 percent (by weight) to saturated.
- Hydrostatic stress: 0 to 20 MPa.
- Stress difference: 0 to 5 MPa.
- Kinematic and static quantities: all known or measured.

When these criteria were applied to the data acquired from the tests on crushed salt and crushed-salt mixtures, the data from only five studies [Holcomb and Hannum, 1982; Pfeifle and Senseny, 1985; Holcomb and Shields, 1987; Zeuch et al., 1991; and Brodsky, 1994] were accepted for use in the constitutive model development. These five studies represent 81 tests, which include 17 hydrostatic compaction tests, 53 hydrostatic consolidation tests, and 11 triaxial compression shear consolidation tests. In a hydrostatic compaction test, a right-circular, cylindrically-shaped specimen is loaded by increasing the magnitude of the three principal stresses at equivalent and uniform rates until a specified stress level is achieved. During the test, both the principal stresses and either the density or the volumetric strain are measured. In a hydrostatic consolidation test, a right-circular, cylindrical specimen is hydrostatically loaded to a specified hydrostatic stress level, and then the hydrostatic stress is maintained at the specified level for a prescribed period of time. During the consolidation stage (i.e., the period following load up), the volumetric strains (density) are measured continuously. In a triaxial compression shear consolidation test, a right-circular, cylindrical specimen is first loaded hydrostatically to a specified hydrostatic stress level, and then a stress difference is applied by rapidly increasing the axial stress to a specified level above the hydrostatic stress. The stress state is then maintained for a prescribed period of time. The hydrostatic stress level may correspond to either the mean stress or the confining pressure in the shear consolidation stage. During the consolidation period, the axial and volumetric strains are measured continuously.

The 17 hydrostatic compaction tests are quasi-static tests; therefore, they were not included in the database to determine the parameter values for the creep consolidation models. In addition, only the first stage of multistage tests were retained because the initial and postload densities were not well defined for the subsequent stages. Removing these tests left 52 tests in the database, which includes 40 hydrostatic consolidation tests and 12 shear consolidation tests.

PARAMETER EVALUATION

A fundamental component of the constitutive model evaluation process includes the ability of each of the models to reproduce laboratory-measured responses. The constitutive models were fit to the laboratory data to determine the model parameters such that the square of the difference between the laboratory-measured and model-predicted response was minimized. Application of the least-squares fitting criterion to

the constitutive models requires solution of simultaneous nonlinear equations. These complex nonlinear equations were solved with the BMDP statistical software package [Frane et al., 1985].

Two different types of laboratory test responses were used in the least-squares fitting: hydrostatic consolidation tests and shear consolidation tests. No information can be obtained about the deviatoric portion of the models from the hydrostatic consolidation database because the deviatoric stress (stress difference) is zero in these experiments. However, the five flow potential parameter values can be determined independent of the particular model if the ratio of lateral to axial strain rate is fit to the ratios from the shear consolidation tests. The temperature, moisture content, and particle size variations in the shear consolidation experimental database are insufficient to obtain information regarding these variables. Therefore, parameter values for ξ in Equation 9 were obtained from the hydrostatic consolidation tests. Details of the model fitting procedure can be found in Callahan et al. [1995]. Parameter values obtained by fitting the lateral to axial strain rate ratios from the shear consolidation tests are given in Table 1. Although the parameter D_t also appears in the flow potential, it cannot be determined uniquely since it also appears in the effective stress in the equivalent strain rate measures. Figure 1 illustrates the lateral to axial strain rate ratios and the flow potential predictions for a typical test. The test specimen reached a final density of 2,135 kg/m^3; thus, the predicted values were projected to the intact density of 2,160 kg/m^3.

Table 1. Parameter Values for Flow Potential

Parameter	Units	Value
κ_0	MPa$^{1-\kappa_2}$	4.430
κ_1	—	0.233
κ_2	—	1.984
m_2	—	2.170
σ_{r_2}	MPa	0.823

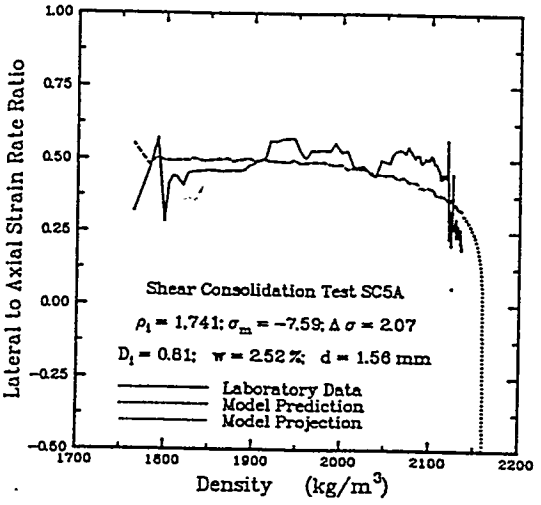

Figure 1. Laboratory and Predicted Lateral to Axial Strain Rate Ratios.

Table 2 lists the parameter values obtained for the modified Sjaardema and Krieg, the modified Zeuch, and the modified Spiers models. Values for parameters that have not been masked by our model changes are compared with the values proposed by the referenced researchers. Figures 2 and 3 compare the model predictions for two laboratory tests. The specimen in Figure 2 had an initial density of 1,665 kg/m^3, added moisture of 2.33 percent by weight, and a mean particle size of 1.56 mm and was subjected to a compressive mean stress of 5.63 MPa and a stress difference of 1.38 MPa for a period of 65 days. Figure 2 represents one of the better comparisons of the model

predictions of the experimental data. The specimen data shown in Figure 3 had an initial density of 1,808 kg/m^3, no added moisture, and a mean particle size of 1.56 mm and was subjected to a compressive mean stress of 2.67 MPa and a stress difference of 5.0 MPa for a period of 28 days. Figure 3 represents one of the least favorable comparisons of the model predictions to the test data. The interesting feature to compare between Figures 2 and 3 is the lateral strain components. In Figure 2, the lateral strain is directed inward and contributing to the consolidation of the specimen. However, in Figure 3, the lateral strain is directed outward, and the net volumetric consolidation is in the axial direction. The predictions of the creep consolidation models included in the figures show that the models are able to capture this important change in behavior (i.e., reversal in direction of the lateral strain component).

Table 2. Parameter Values for the Crushed-Salt Models

Parameter	Units	Modified Material Model			Reference Values
		Sjaardema and Krieg	Zeuch	Spiers	
η_0	$(MPa)^{1-\eta_2}$	−1.437	−42.33	$-2.91(10^{-6})$	—
η_1	—	2.594	2.740	0.108	—
η_2	1/MPa	3.623	3.049	5.523	—
m_1	—	0.731	0.605	0.174	—
σ_{r_1}	—	3.535	18.33	0.019	—
D_t	—	0.867	0.888	0.881	—
a_1	—	17.00	20.10	71.10	—
a_2	—	$4.75(10^3)$	$9.66(10^3)$	62.6	—
Q_c/R	K	$4.01(10^3)$	$9.26(10^{-17})$	$1.8(10^2)$	—
p	—	0.564	0.396	$3.22(10^{-5})$	—
B_0	$kg \cdot m^{p-3}/(MPa \cdot s)$	$6.459(10^7)$			—
A	m^3/kg	$-1.307(10^{-2})$			$-1.72(10^{-2})$
b_2	—		4.469		1/3
b_3	—		5.722		1/2
b_7	$m^p/(MPa \cdot s)$		$6.54(10^{-14})$		—
b_8	$m^p/(MPa \cdot s)$		$9.05(10^{-19})$		—
n	—		9.991		4.9
r_1	$m^p/(MPa \cdot s)$			$1.02(10^{-7})$	—
r_3	—			9.770	1/3
r_4	—			0.806	2
n	—			3.190	4.15

WIPP SHAFT EXAMPLE PROBLEM

Crushed salt is proposed as a shaft seal component between 430 m and 600 m in depth. Current designs specify that crushed salt be dynamically compacted so that the initial fractional density will be about 0.9. As the host salt formation creeps inward with time, the crushed salt is expected to consolidate and heal to form a seal as

impermeable as the host salt formation. The fractional density of the crushed salt as a function of depth and time is of interest. The fractional density is related to the permeability of the crushed salt indirectly through other laboratory experiments that have measured permeability at various fractional densities of consolidated crushed salt. Numerical models of the shaft provide fractional densities of the compacted salt column as a function of depth and time so that permeability of the compacted salt seal component is known as a function of depth and time. The creep consolidation models presented here have been implemented into the finite element thermomechanical stress analysis program SPECTROM-32 [Callahan et al., 1989].

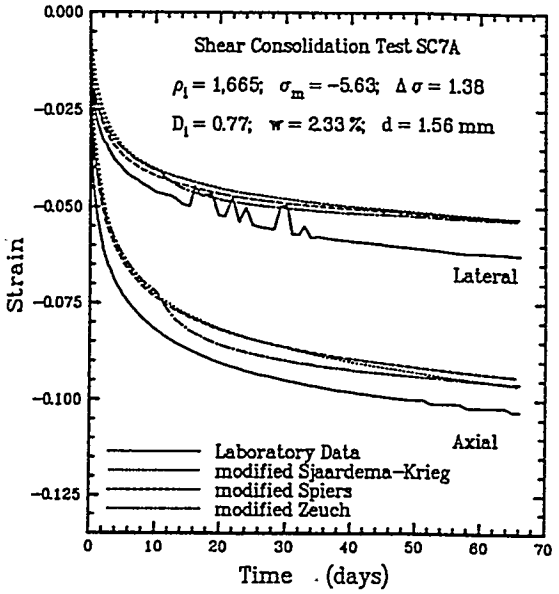

Figure 2. Comparison of Model Predictions and Experimental Data.

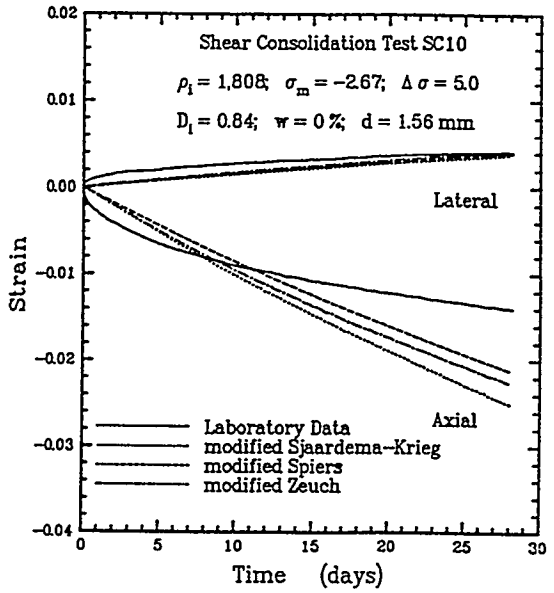

Figure 3. Comparison of Model Predictions and Experimental Data.

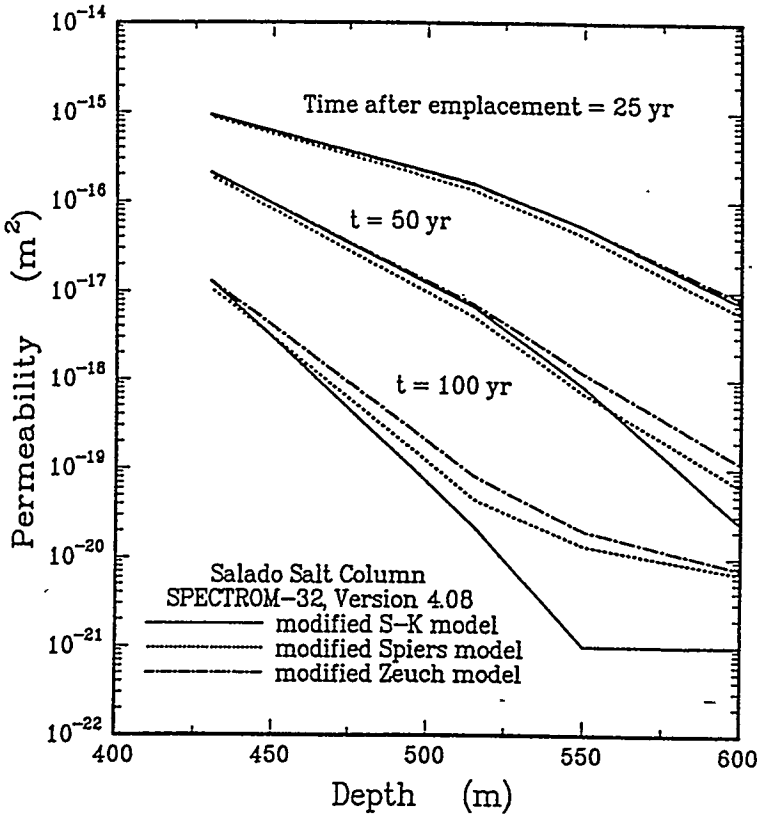

Figure 4. Permeability in a Crushed-Salt Shaft Seal Component.

To examine the consolidation of crushed salt emplaced in a shaft, a section of the shaft was modeled in axially-symmetric geometry assuming plane-strain conditions along the axis of the shaft. A constitutive model for inelastic flow and damage evolution (MDCF model) for argillaceous salt [Chan et al., 1994] was used to predict the behavior of the rock mass surrounding the shafts. The construction sequence assumes that the shaft is excavated instantaneously and left open for 50 years before crushed salt is tamped in place. Shaft closure and consolidation of the compacted salt were simulated for 150 years or 100 years after the crushed salt is emplaced. Fractional density is related to permeability by $\log_{10}k = -66.67(D - 1) - 21$ m^2, which is known as the Knowles-Hansen relationship for crushed salt [Department of Energy, 1995]. Figure 4 shows the permeability as a function of depth in the crushed salt. The curves show that the lower portion of the crushed-salt seal component attains low permeability after 100 years and fully consolidates for one model (S-K) reaching the assumed permeability of the host formation (10^{-21} m^2).

CONCLUSIONS

This paper examines the mechanical behavior of crushed salt, which is to be used as a long-term seal component for the shafts at the WIPP site. Three models were selected for evaluation; i.e, those attributed to Sjaardema–Krieg, Zeuch, and Spiers. The models were generalized to three-dimensional forms and modified where deemed necessary. A database comprised of hydrostatic and shear consolidation tests was created and used to determine the material parameters of the candidate constitutive

models. Rank ordering of the statistical measures obtained from the model fitting indicates that the modified Spiers' model is moderately superior to the other two models. The new stress dependence and generalization enable the models to represent crushed-salt behavior under deviatoric stresses.

The modified Zeuch model (dislocation mechanisms) is based on work performed on dry crushed salt. The modified Spiers model (diffusional transport mechanisms) is based on work performed on wet crushed salt. A comprehensive model should be developed that includes contributions from both types of densification mechanisms. In essence, the modified Zeuch model and the modified Spiers model should be combined or, alternatively, the diffusional process could be added to the modified Zeuch model as outlined by Zeuch [1990]. The initial strain rates predicted by both the modified Zeuch and Spiers models are very sensitive to the selection of the starting conditions, which need to be better defined. As shown in Figure 3, the initial transient behavior of the crushed salt is not captured very well for higher initial densities. This could potentially be improved by describing the transient behavior similar to the model used for intact salt.

The experimental database presently includes only constant-stress types of tests. The database could be improved with the addition of data from multiple load paths (e.g., constant strain rate tests). In addition, the number of tests conducted should be expanded with a wider range of temperature, moisture, and particle size to capture the influence of these variables.

ACKNOWLEDGEMENTS

Work for this study was conducted through Sandia National Laboratories, a Department of Energy facility, and supported by the Department of Energy, Contract DE-AC04-94AL85000.

REFERENCES

Brodsky, N. S., 1994. *Hydrostatic and Shear Consolidation Tests With Permeability Measurements on Waste Isolation Pilot Plant Crushed Salt,* SAND93-7058, prepared by RE/SPEC Inc., Rapid City, SD, for Sandia National Laboratories, Albuquerque, NM.

Callahan, G. D., M. C. Loken, L. L. Van Sambeek, R. Chen, T. W. Pfeifle, J. D. Nieland, and F. D. Hansen, 1995. *Evaluation of Potential Crushed-Salt Models,* SAND95-2143, prepared by RE/SPEC Inc., Rapid City, SD, for Sandia National Laboratories, Albuquerque, NM.

Callahan, G. D., A. F. Fossum, and D. K. Svalstad, 1989. *Documentation of SPECTROM-32: A Finite Element Thermomechanical Stress Analysis Program,* DOE/CH10378-2, prepared by RE/SPEC Inc., Rapid City, SD, RSI-0269, for the U. S. Department of Energy, Chicago Operations Office, Argonne, IL, Vol. 1 and 2.

Chan, K. S., N. S. Brodsky, A. F. Fossum, S. R. Bodner, and D. E. Munson, 1994. "Damage-Induced Nonassociative Flow in Rock Salt," *International Journal of Plasticity,* Vol. 10, pp. 623–642.

Department of Energy, 1995. *Waste Isolation Pilot Plant Sealing System Design Report,* DOE/WIPP-95-3117, Waste Isolation Pilot Plant, October.

Fossum, A. F., G. D. Callahan, L. L. Van Sambeek, and P. E. Senseny, 1988. "How Should One-Dimensional Laboratory Equations be Cast Into Three-Dimensional Form?," *Proceedings, 29th U.S. Symposium on Rock Mechanics, June 13–15, University of Minnesota, Minneapolis, MN,* A. A. Balkema, Rotterdam, pp. 35–41.

Frane, J. W., L. Engelman, and J. Toporek, 1985. *BMDP Programmer's Guide and Subroutine Writeups: Documentation of the FORTRAN Source; Part I. Programmer's Guide; Part II. Subroutine and Common Block Writeups,* BMDP Technical Report No. 55.

Holcomb, D. J. and D. W. Hannum, 1982. *Consolidation of Crushed Salt Backfill Under Conditions Appropriate to the WIPP Facility,* SAND82-0630, Sandia National Laboratories, Albuquerque, NM.

Holcomb, D. J. and M. E. Shields, 1987. *Hydrostatic Creep Consolidation of Crushed Salt With Added Water,* SAND87-1990, Sandia National Laboratories, Albuquerque, NM.

Munson, D. E., A. F. Fossum, and P. E. Senseny, 1989. *Advances in Resolution of Discrepancies Between Predicted and Measured In Situ WIPP Room Closures,* SAND88-2948, Sandia National Laboratories, Albuquerque, NM.

Pfeifle, T. W. and P. E. Senseny, 1985. *Permeability and Consolidation of Crushed Salt From the WIPP Site,* RSI-0278, prepared by RE/SPEC Inc., Rapid City, SD, for Sandia National Laboratories, Albuquerque, NM.

Sjaardema, G. D. and R. D. Krieg, 1987. *A Constitutive Model for the Consolidation of WIPP Crushed Salt and Its Use in Analyses of Backfilled Shaft and Drift Configurations,* SAND87-1977, Sandia National Laboratories, Albuquerque, NM.

Spiers, C. J. and R. H. Brzesowsky, 1993. "Densification Behaviour of Wet Granular Salt: Theory Versus Experiment," *Proceedings, Seventh Symposium on Salt,* Vol. I, pp. 83–92, Elsevier Science Publishers B.V., Amsterdam.

Xu, J. and R. M. McMeeking, 1995. "Finite Element Simulation of Powder Consolidation in the Formation of Fiber Reinforced Composite Materials," *International Journal of Mechanical Science,* Vol. 37, No. 8, pp. 883–897.

Zeuch, D. H., 1990. "Isostatic Hot-Pressing Mechanism Maps for Pure and Natural Sodium Chloride: Applications to Nuclear Waste Isolation in Bedded and Domal Salt Formations," *International Journal of Rock Mechanics and Mineral Sciences & Geomechanical Abstracts,* Vol. 27, pp. 505–524.

Zeuch, D. J., D. J. Zimmerer, and M. E. Shields, 1991. *Interim Report on the Effects of Brine-Saturated and Shear Stress on Consolidation of Crushed, Natural Rock Salt From the Waste Isolation Pilot Plant (WIPP),* SAND91-0105, Sandia National Laboratories, Albuquerque, NM.

DISCLAIMER